

# RobotDancing: Residual-Action Reinforcement Learning Enables Robust Long-Horizon Humanoid Motion Tracking

Zhenguo Sun<sup>1,2\*</sup>, Yibo Peng<sup>2\*</sup>, Yuan Meng<sup>1</sup>, Xukun Li<sup>1</sup>, Bo-Sheng Huang<sup>3</sup>,  
Zhenshan Bing<sup>4†</sup>, Xinlong Wang<sup>2†</sup>, Alois Knoll<sup>1</sup>

**Abstract**—Long-horizon, high-dynamic motion tracking on humanoids remains brittle because absolute joint commands cannot compensate model–plant mismatch, leading to error accumulation. We propose RobotDancing, a simple, scalable framework that predicts residual joint targets to explicitly correct dynamics discrepancies. The pipeline is end-to-end—training, sim-to-sim validation, and zero-shot sim-to-real—and uses a single-stage reinforcement learning (RL) setup with a unified observation, reward, and hyperparameter configuration. We evaluate primarily on Unitree G1 with retargeted LAFANI dance sequences and validate transfer on H1/H1-2. RobotDancing can track multi-minute, high-energy behaviors (jumps, spins, cartwheels) and deploys zero-shot to hardware with high motion tracking quality.

## I. INTRODUCTION

Humanoid robots are increasingly expected to execute long-horizon, highly dynamic behaviors such as dance, where small tracking errors compound rapidly and destabilize control. A principal source of such drift is the mismatch between idealized reference trajectories and the robot’s true physics (actuation limits, friction, inertia, latency). Since the field of animation has shown incredible progress in whole body dynamic control of physics-based characters [1], [2], [3], precise and robust motion tracking has been one of the core challenges in humanoid robotics, particularly when transferring motions from simulation or captured human data to real-world robotic platforms.

Recent advances in physics-based humanoid control [4], [5], [6], [7], [8], [9], [10], [11] have demonstrated the potential of learning-based controllers integrated with physical constraints. Nevertheless, most existing methods generally still predict absolute joint commands, which works well for short, quasi-cyclic skills but remains fragile on long, high-energy sequences, leaving untapped the potential of explicitly modeling and compensating for dynamic discrepancies.

Inspired by residual learning paradigms [12], [13], we propose a novel residual-action reinforcement learning (RL) framework **RobotDancing** for high-quality tracking of long high-dynamic dance motions. Unlike previous methods, our framework explicitly learns the dynamics discrepancy between the reference motion and the robot. Instead of issuing

absolute commands, the policy outputs residual actions that correct the reference in joint space, thereby allocating model capacity to physics compensation rather than re-synthesizing the motion. This strategy markedly reduces the accumulation of motion tracking errors and enables robust and accurate motion tracking over long horizons.

Our preliminary experiments conducted on the Unitree G1 humanoid robot platform demonstrate notably superior tracking accuracy compared to absolute actions methods, while yielding high motion quality. Furthermore, we also validated our framework’s generalization capabilities across multiple humanoid robot platforms (Unitree H1 and H1-2).

The primary contributions of this paper include:

- **A Simple, Open, and Scalable Motion-Tracking Framework.** We present an end-to-end pipeline—training, sim-to-sim validation, and sim-to-real deployment—that achieves long-horizon, high-dynamic tracking with a single-stage RL algorithm (no multi-stage distillation or teacher-student schemes [14]).
- **Residual-Action Tracking Targets Dynamics Discrepancy.** A residual-action policy corrects reference joints online, reducing error accumulation and improving stability on demanding sequences (e.g., dance).
- **Effective Sampling for Long-Tail Motions.** A two-part strategy (distribution-aware balancing + failure-aware prioritization) improves coverage of rare but informative poses and accelerates progress on difficult segments.
- **Generalization across Motions and Platforms.** A unified set of observations, rewards, and hyperparameters trains diverse motions without per-task tuning, and transfers to multiple humanoid platforms including 2 full-size robots; to the best of our knowledge, this is one of the first demonstrations of high-dynamic, long-horizon motion tracking on full-size humanoids.

## II. RELATED WORK

### A. Motion Tracking for Humanoids

Learning-based control has achieved impressive results on task-specific humanoid skills such as locomotion, balancing, and getting up [15], [16], [17], [18], yet these controllers typically rely on careful reward engineering and often yield motions that are not consistently human-like. By contrast, motion tracking seeks to reproduce human demonstrations, providing a direct route to natural whole-body behaviors.

*Single-skill tracking.* DeepMimic [1] established the canonical formulation in simulation, demonstrating that

\* Equal contribution. † Corresponding author.

<sup>1</sup>School of Computation, Information and Technology, Technical University of Munich, 85748 Munich, Germany.

<sup>2</sup>Beijing Academy of Artificial Intelligence, 100084 Beijing, China.

<sup>3</sup>Department of Computer Science, Tsinghua University, 100084 Beijing, China.

<sup>4</sup>The State Key Laboratory for Novel Software Technology, Nanjing University, 215163 Suzhou, China.

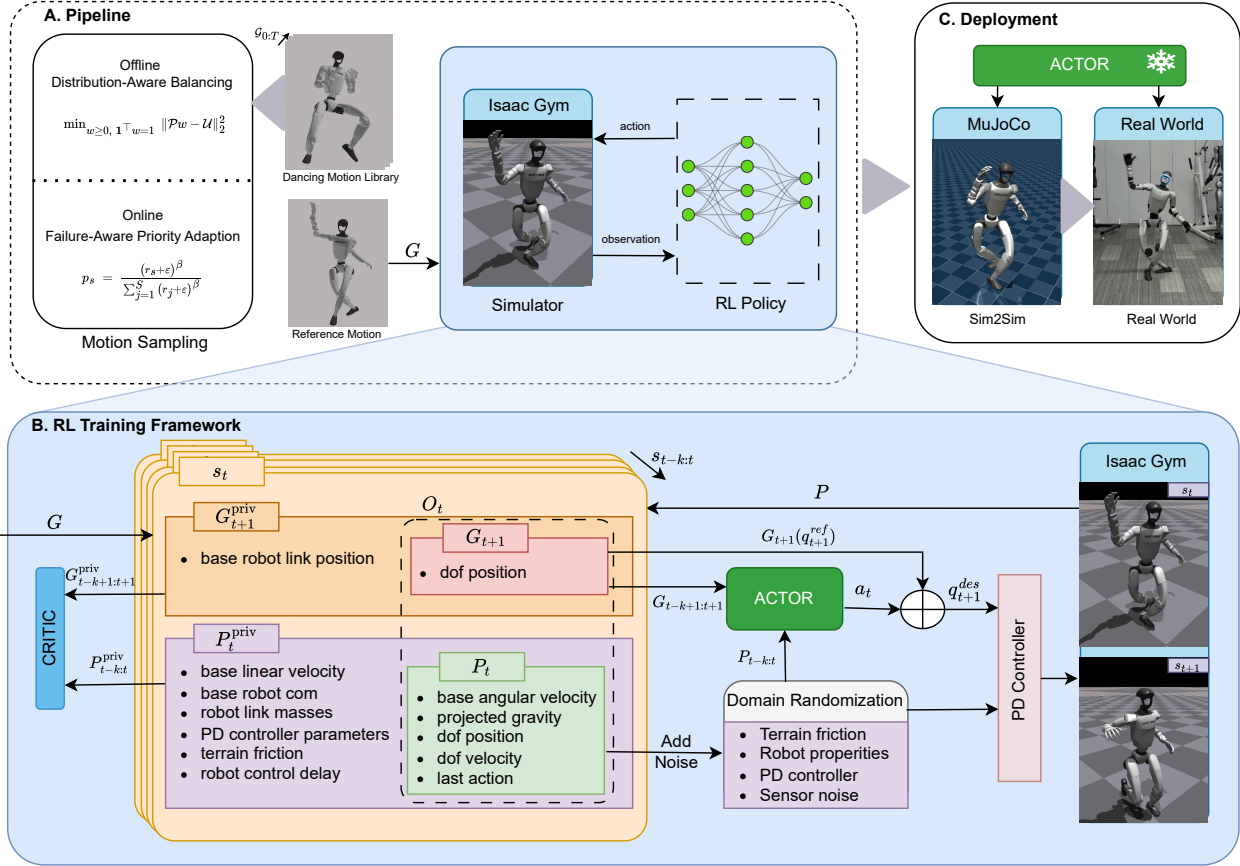


Fig. 1. **Framework of RobotDancing.** (a) The pipeline from motion data processing to RL policy learning. (b) The RL training framework for long-horizon high-dynamic motion tracking tasks through residual action learning. (c) The deployment framework enables Sim2Sim and Sim2Real transfers.

reference-conditioned policies can reproduce diverse skills under physics constraints. Subsequent systems extended this paradigm to whole-body humanoids and toward reality: ASAP [5] aligned simulation and real-world physics for agile skills via careful modeling and randomization; Kung-fuBot [4] integrated whole-body control with curriculum and domain randomization to acquire highly dynamic behaviors; and HoST [17] learned to stand up across diverse postures further stressed robustness under large disturbances.

**General motion tracking and teleoperation.** Recent systems pursue broader motion coverage: ExBody2 [6] advances expressive whole-body control, and OmniH2O [7] combines teleoperation and learning toward universal control; PHC [19] targets long-lived avatar tracking in simulation. A complementary line emphasizes whole-body teleoperation for mobile manipulation (often upper-body dominant), e.g., TWIST [20], CLONE [21], HOMIE [22], and AMO [23]. These frameworks typically depend on specialized interfaces, multi-stage pipelines, or hand-tuned objectives, and only partially address long-horizon stability.

**Long-horizon tracking.** Long-horizon tracking is particularly challenging due to error accumulation and reference–robot mismatch. A recent effort, BeyondMimic [24],

achieves long-sequence execution via guided diffusion and sophisticated sampling/reset strategies. While effective, this method primarily addresses where to sample along the trajectory and how to stitch segments; it still treats the action as an absolute command relative to the reference.

### B. Residual Learning in Robotics

Residual learning (adding a learned correction on top of a nominal policy/controller) has been explored across robot domains. Residual RL has improved contact-rich manipulation and locomotion by refining model-based or hand-designed controllers [13], [25], and has been combined with feedback structures for bipedal systems such as Cassie [26]. Fine-grained whole-body controllers also employ residual terms to enhance accuracy on selected subsystems (e.g., upper-body manipulation in ULC [27]). Closest to our scope, I-CTRL [12] uses residual actions for humanoid motion tracking in simulation with constrained RL, indicating that residualization can stabilize imitation.

### C. Discussion and Our Focus

In practice, reference motions for humanoids are commonly obtained by retargeting human demonstrations; they are kinematically consistent with the human but generally

not dynamically consistent with the robot. Consequently, absolute-action trackers tend to accumulate errors and fail on long, high-dynamic sequences. We explicitly address this gap by: (i) learning residual actions that specialize in compensating robot–reference dynamics discrepancies, thereby reducing long-horizon drift; and (ii) introducing a two-stage sampling scheme—distribution-aware balancing and failure-aware prioritization—that increases coverage of rare yet informative poses and allocates training to persistently difficult segments. Together, these design choices yield a simple, scalable, and single-stage RL pipeline that achieves high-fidelity, long-horizon tracking and transfers across full-size humanoid platforms.

### III. METHOD

We present **RobotDancing**: a *scalable training paradigm for residual-dynamics motion tracking* that is capable of tracking long-horizon, highly dynamic motions (e.g., dance). As illustrated in Fig. 1, a motion library provides reference trajectories; a goal-conditioned RL policy outputs residual actions on top of the references, which are executed by a low-level joint-space PD controller. Training combines *distribution-aware* and *failure-aware* motion resampling, *phase-free reference conditioning*, *selective residual actions*, *curriculum learning*, and *domain randomization* for robustness and generalization. This section is organized as follows: Sec. III-A formalizes the problem and notations; Sec. III-B introduces the whole RL training framework; Sec. III-C details our motion sampling strategy; Sec. III-D specifies residual action learning; Sec. III-E presents curriculum scheduling; Sec. III-F describes domain randomization.

#### A. Problem Formulation and Notation

We consider motion tracking task as a discrete-time partially observable Markov decision process (POMDP) with state space  $\mathcal{S}$ , observation space  $\mathcal{O}$ , reference motions  $\mathcal{G}_{0:T}$ , action space  $\mathcal{A}$ , and transition  $p(s_{t+1} | s_t, a_t)$ . As illustrated in Fig. 1, we use the following symbols:

- **System state**  $s_t \in \mathcal{S}$ : the full physical state of the robot and environment at time  $t$  (unobserved).
- **Proprioception**  $P_t$ : robot onboard measurements derived from  $s_t$ , e.g., joint positions/velocities, base linear/angular velocity, projected gravity, last action;  $P_t$  and  $P_t^{\text{priv}}$  represent the basic proprioception and privileged information, respectively.
- **Motion library & reference**  $G \in \mathcal{G}_{0:T}$ : a time-indexed repository of reference frames. At step  $t$ , we retrieve  $G_{t+1}$ , which provides joint-space targets and kinematic context (e.g., joint positions/velocities and link poses). We denote the joint references by  $G_{t+1}$  and the privileged quantities by  $G_{t+1}^{\text{priv}}$ .
- **Observation**  $O_t$ : constructed by concatenating proprioception  $P_t$  with the reference  $G_{t+1}$ ,

$$O_t = \Psi(P_t, G_{t+1}) \triangleq [P_t ; G_{t+1}] \in \mathcal{O}, \quad (1)$$

where  $\Psi(\cdot, \cdot)$  denotes the concatenation operator.

- **Action**  $a_t \in \mathbb{R}^{23}$ : the target residual joint position for the PD controller to calculate motor torques.

### B. RL Training Framework

**Goal-Conditioned RL.** We employ a goal-conditioned formulation in which the goal  $g_t$  is derived from the reference:  $g_t = G_{t-k+1:t+1}$ , the proprioception observation  $o_t$  is:  $o_t = P_{t-k:t}$ , where  $k$  means a short look-back window size. The policy then maps observation and goal to actions:

$$a_t \sim \pi_\theta(a_t | o_t, g_t), \quad (2)$$

and reduces to the standard partially observed policy when the goal is omitted:  $\pi_\theta(a_t | O_{t-k:t})$ .

**Asymmetric Actor-Critic.** We adopt an asymmetric actor-critic architecture based on the standard PPO algorithm [28] similar to most previous works [1], [4], [5] in which the actor is trained with the partial observation and the critic with an augmented observation. Unlike [4], [5], we do not introduce an explicit time-phase variable; instead, the policy is conditioned on the reference joints directly. The input of the actor is  $O_{t-k:t} = [P_{t-k:t}; G_{t-k+1:t+1}]$  with stacked  $k$  timesteps of proprioception  $P_t = [q_t, \dot{q}_t, g_t^{\text{proj}}, \omega_t^{\text{base}}, a_{t-1}]$  where  $q_t, \dot{q}_t \in \mathbb{R}^{23}$  denote joint positions and velocities,  $g_t^{\text{proj}} \in \mathbb{R}^3$  encodes the base orientation through projected gravity,  $\omega_t^{\text{base}} \in \mathbb{R}^3$  is the base angular velocity, and  $a_{t-1}$  is residual actions in the last timestep, and the reference  $G_{t+1} = [q_{t+1}^{\text{ref}}]$  where  $q_{t+1}^{\text{ref}} \in \mathbb{R}^{23}$  is the absolute joint position reference for the next timestep. The critic receives an augmented observation  $O_{t-k:t}^{\text{priv}} = [O_{t-k:t}, v_{t-k:t}^{\text{base}}, p_{t-k+1:t+1}^{\text{link,ref}}, \xi_{t-k:t}]$  where  $v_{t-k:t}^{\text{base}}$  is the base linear velocity,  $p_{t+1}^{\text{link,ref}} \in \mathbb{R}^{27}$  is the calculated base robot link position references for the next timestep, and  $\xi_t$  stacks randomized physical parameters (e.g., friction, masses/inertias, PD gains, delays) for value conditioning. At test time, only  $O_{t-k:t}$  is required.

**Residual Actuation.** Instead of predicting absolute joint commands, the policy outputs residual actions on top of the reference in joint space. Let the commanded joint target be

$$q_t^{\text{tar}} = q_{t+1}^{\text{ref}} + a_t, \quad (3)$$

$$\tau_t = \text{PD}(q_t^{\text{tar}}, q_t, \dot{q}_t), \quad (4)$$

where  $\text{PD}(\cdot)$  denotes a low-level joint-space controller. This design assigns kinematic consistency to the reference  $G_{t+1}$ , while allowing the policy to focus on compensating dynamics discrepancies between the robot and the reference.

**Rewards.** Following prior work [4], [29], we vectorize both the reward and the value function to decouple heterogeneous objectives (e.g., imitation and physical regularization). At each step  $t$ , we define  $\mathbf{r}_t = [r_t^{(1)}, \dots, r_t^{(n)}] \in \mathbb{R}^n$  and  $\mathbf{V}_\phi(s) = [V_\phi^{(1)}(s), \dots, V_\phi^{(n)}(s)]$  where a single critic network with a shared trunk and  $n$  output heads estimates per-component values. This design avoids premature scalarization of rewards, yields more precise value estimates per objective, and improves the stability of policy optimization under heterogeneous magnitudes and schedulable priorities.

We design rewards in a modular way to remain simple and scalable while matching our motion tracking objective. Specifically, we factorize the rewards into a task (motion tracking) part and a regularization part:

$$r_t = r_t^{\text{track}} - s_{\text{pen}}(t) r_t^{\text{reg}}, \quad (5)$$

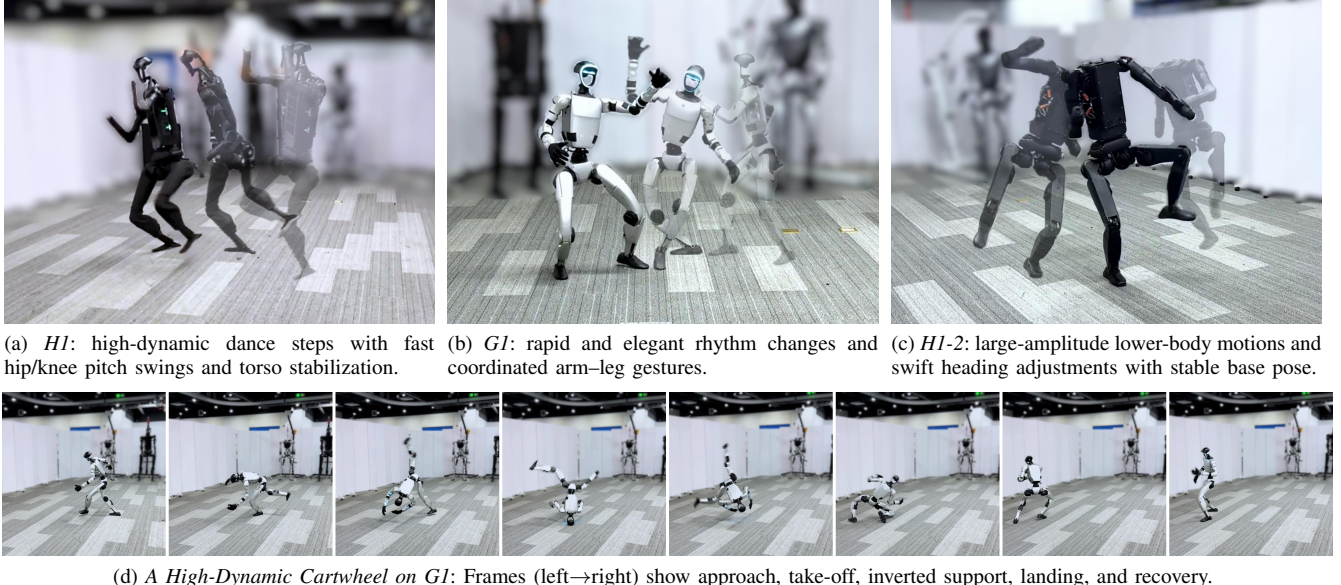


Fig. 2. **Real-World High-Dynamic Motions across Platforms.** Multiple platforms perform long-horizon, high-dynamic dance sequences. Motion trails visualize stable tracking over time; the same residual-action framework applied on all platforms without task-specific retuning.

where  $s_{\text{pen}}(t) \in [s_{\min}, s_{\max}]$  is a curriculum-controlled penalty scale, as described in [4], [5].

**Task (Motion Tracking).** We follow a DeepMimic-style [1] shaping that combines a small set of task-space and joint-space errors with Gaussian kernels:

$$r_t^{\text{track}} = \sum_{\chi \in \mathcal{C}} w_{\chi} \exp(-\bar{e}_{\chi}(t) / \sigma_{\chi}^2), \quad (6)$$

where  $\mathcal{C}$  includes a compact set of pose/velocity terms (e.g., root/EE poses and twists) and joint terms (positions/velocities). Each  $\bar{e}_{\chi}$  is an averaged squared error over the corresponding targets, and  $\sigma_{\chi}$  is a nominal tolerance (fixed or slowly adapted as in [4]). All task terms are positive and uniformly interpretable across skills.

**Regularization.** We keep regularization minimal to avoid hurting motion tracking while ensuring physical plausibility:

$$\begin{aligned} r_t^{\text{reg}} = & \lambda_{\tau} \|\tau_t\|_2^2 + \lambda_{\Delta a} \|a_t - a_{t-1}\|_2^2 \\ & + \lambda_{\text{lim}} \mathcal{P}_{\text{soft-limits}}(q_t, \dot{q}_t, \tau_t) + \lambda_{\text{cnt}} \mathcal{P}_{\text{contacts}}(t) \\ & + \lambda_{\text{term}} \mathbb{1}\{\text{collision/termination}\}. \end{aligned} \quad (7)$$

Here  $\|\tau_t\|_2^2$  discourages excessive torques,  $\|a_t - a_{t-1}\|_2^2$  promotes smooth control,  $\mathcal{P}_{\text{soft-limits}}$  softly penalizes approaching joint/velocity/torque limits, and  $\mathcal{P}_{\text{contacts}}$  moderates undesirable contact behavior (e.g., slip/stumble or excessive contact forces). In addition, the indicator term  $\mathbb{1}\{\text{collision/termination}\}$  activates when a self-/environment collision or a safety-critical termination (e.g., a fall or hard limit violation) occurs, applying a large terminal penalty at that timestep to discourage unsafe behaviors and prematurely end the episode. Only a few coefficients  $\{\lambda\}$  are used and scheduled by the same curriculum as  $s_{\text{pen}}(t)$ .

This factorization isolates *what to imitate* (Eq. (6)) from *how to stay physically plausible* (Eq. (7)), stabilizing PPO updates and improving long-horizon tracking. All reward weights are tuned once and reused across different tasks.

### C. Motion Sampling Strategy

For reference frame sampling, we employ a two-stage resampling strategy that improves sample efficiency while preserving coverage: an *offline distribution-aware balancing* and an *online failure-aware priority adaptation*.

**Distribution-Aware Balancing.** Locomotion such as walking/running is near-cyclic [30], whereas long-horizon, high-dynamic motions (e.g., dance) exhibit strong inter-/intra-motion variability. As shown in Fig. 3, key lower-body joints display much larger dispersion across segments and motions, making uniform sampling ineffective. Empirically, *hip/knee pitch* dominate this variability, while *hip roll/yaw* and other robot joints remain near neutral. Hence balancing focuses on the pitch subspace, reducing dimensionality and concentrating effort on informative DOFs.

Offline, motion clips are partitioned into temporal segments and binned in the selected key DOFs derived from the motion analysis to form occupancy histograms. Sampling weights are then obtained by matching a uniform target:

$$\min_w \|\mathcal{P}w - \mathcal{U}\|_2^2, \quad \text{s.t. } \sum_i w_i = 1, \quad w_i \geq 0 \quad (8)$$

where  $\mathcal{P}$  stacks per-segment occupancies,  $\mathcal{U}$  is the uniform target, and  $w$  are segment weights. This equalizes over-represented poses and increases coverage of rare but discriminative configurations, improving early-stage learning without sacrificing diversity. The result is depicted in Fig. 4. In practice, the environment alternates between reference-index sampling and the balanced sampler to retain temporal coherence while avoiding mode bias.

**Failure-Aware Priority Adaptation.** In long sequences the difficulty is highly nonuniform: policies quickly master “comfort zones” while repeatedly failing in “unstable windows”. Purely uniform time sampling (e.g. [4], [5], [19])

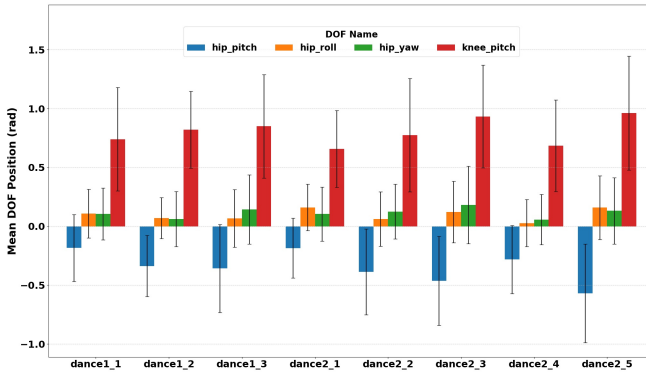


Fig. 3. **Mean and Standard Deviation of Lower-Body Joint Angles Across Dance Motions.** Long-horizon, high-dynamic dance motions exhibit pronounced inter-motion-segment differences and large variance in key lower-body joint positions.

therefore over-revisits easy segments and starves rare, error-prone ones, which inflates gradient noise and slows progress on the true bottlenecks. We treat difficulty as a streaming signal indexed by the start time of a segment and estimate it online, similar to the method introduced in [9].

**Formulation.** Partition each motion into  $S$  one-second segments. For segment  $s$ , maintain an EMA stability score using terminal outcomes,

$$r_s^{(t+1)} = (1 - \alpha) r_s^{(t)} + \alpha f_s^{(t)}, \quad f_s^{(t)} \in \{0, 1\},$$

and we define a tempered difficulty prior

$$p_s = \frac{(r_s + \varepsilon)^\beta}{\sum_{j=1}^S (r_j + \varepsilon)^\beta}, \quad (9)$$

where  $f_s^{(t)}$  indicates if the motion segment  $s$  is failed in the iteration  $t$ ,  $\alpha$  is the EMA factor, and  $\beta$  controls the hardness.

Offline balancing addresses the intrinsic long-tail structure of dance-like motions, while online adaptation progressively allocates more budget to persistently difficult segments. The combination yields broad coverage early and targeted refinement later, leading to faster and more stable training.

**Reference State Initialization (RSI).** In addition, in order to improve the training efficiency further, we adopt RSI [1] to randomize the starting point along the reference trajectory. At the beginning of each episode, we sample a time index  $t \sim \mathcal{G}\{0, \dots, T\}$  from the motion library and reset the simulator state to the corresponding reference state with small jitter:

$$(q_0, \dot{q}_0, x_0^{\text{root}}, \dot{x}_0^{\text{root}}) \leftarrow (q_t^{\text{ref}}, \dot{q}_t^{\text{ref}}, x_t^{\text{root,ref}}, \dot{x}_t^{\text{root,ref}}) + \varepsilon,$$

where  $\varepsilon$  is a small Gaussian perturbation, and  $x^{\text{root}}$  and  $\dot{x}^{\text{root}}$  represent the robot root position and velocity, respectively.

#### D. Residual Action Learning

**Selective Residualization.** Not all DOFs require residuals. For DOFs whose references are statistically stable and low-variance, we pass the reference directly; for error-sensitive and dynamic-demanding DOFs (e.g., pitch joints of knee and

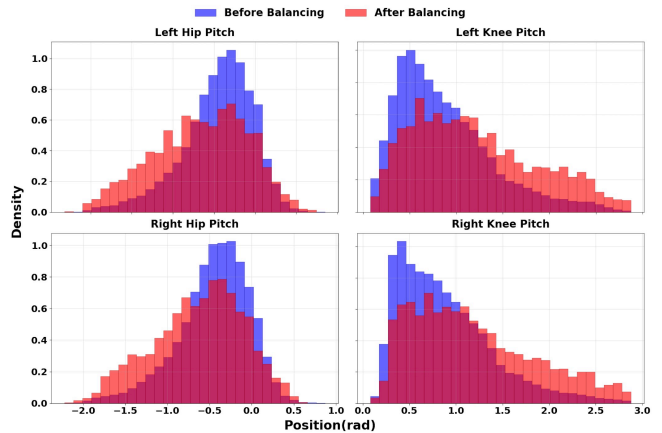


Fig. 4. **Effect of Distribution-Aware Balancing on Key Lower Body Joint Position Distributions.** **Before Balancing** shows the original data distribution, while **After Balancing** denotes the distribution after applying our sampling strategy. The strategy flattens over-represented modes and increases coverage of rare poses, yielding a more uniform key lower-body joint-angle density across motions.

hip), the policy outputs residuals. This sparsifies the action, lowers variance, and reduces error propagation.

**Feasibility and Smoothness.** During training, we apply  $\Pi_C$  to  $(q_t^{\text{tar}}, \tau_t)$  to satisfy joint position/velocity/torque limits, and meanwhile bound per-DOF residual magnitudes by quantiles estimated from data.

#### E. Curriculum Learning

We mainly follow [4] to adopt a progressive curriculum: early training allows larger imitation tolerances and lighter regularization to encourage stable exploration; later stages gradually tighten error thresholds and increase regularization weights to improve precision and physical feasibility.

#### F. Domain Randomization

To improve the policy robustness and realize the sim-to-sim and sim-to-real transfer, domain randomization technology is performed over key physical and actuation factors, including link masses/inertias, terrain friction, motor/PD gains, and small sensing/actuation delays and noise. Before deployment, the learned policy is stress-tested via sim-to-sim evaluation across the randomized parameter distribution. We then deploy the same policy to the real robot without fine-tuning, achieving zero-shot sim-to-real transfer.

## IV. EXPERIMENTS

**Scope.** Unless otherwise stated, all results are reported on the Unitree G1 platform; Unitree H1 and H1-2 are used for cross-platform pipeline and training recipe validation only.

#### A. Implementation Details

**Dataset and Retargeting.** We use the *LAFANI* [31] dance subset as the motion library and the retargeted sequences released by Unitree [32], yielding joint-space references  $G_t = \{q_t^{\text{ref}}\}$  and root poses (positions and quaternions).

**Platforms.** Policies are trained in simulation and evaluated on three Unitree humanoid platforms (G1, H1, and H1-2),

TABLE I  
QUANTITATIVE COMPARISON OF RESIDUAL SETTINGS.

Residual Action	$E_{g\text{-}mpbpe} \downarrow$	$E_{mpbpe} \downarrow$	$E_{mpjpe} \downarrow$	$E_{mpjve} \downarrow$	$E_{mpbve} \downarrow$
NONE(baseline)	574.68 $\pm$ 152.353	109.30 $\pm$ 12.012	1967.98 $\pm$ 242.032	229.92 $\pm$ 15.467	11.73 $\pm$ 0.851
ALL	548.76 $\pm$ 132.643	101.09 $\pm$ 14.036	1730.13 $\pm$ 236.180	<b>222.63</b> $\pm$ 18.717	11.33 $\pm$ 1.027
SELECTIVE (ours)	<b>484.72</b> $\pm$ 147.367	<b>89.41</b> $\pm$ 14.102	<b>1564.00</b> $\pm$ 184.299	225.79 $\pm$ 14.014	<b>11.22</b> $\pm$ 1.025

respectively. All platforms share the same framework and training recipe with a unified observation interface, reward function design, and a low-level joint-space PD controller running at 50 Hz.

**Policy and Training.** We adopt an asymmetric actor-critic with residual-action control. The actor and critic share a trunk MLP with three hidden layers (512–256–128, ReLU [33]). The actor outputs a platform-dependent residual action vector of dimension  $d_{\text{act}} \in \{23, 21, 19\}$  for G1, H1-2, and H1, respectively, while the critic uses multi-head value outputs (one head per reward component). Core PPO hyperparameters are  $\gamma = 0.99$ ,  $\lambda_{\text{GAE}} = 0.95$ ,  $\text{entropy\_coef} = 0.01$ ,  $\text{lr} = 1\text{e-}3$ , and desired.kl = 0.01.

**Termination and Reset.** We adopt concise termination criteria to detect tracking failure or unsafe states, and a reference-aware reset to maintain coverage.

*Termination.* An episode ends if any of the following holds: (i) Global joint tracking failure: the mean joint-position error exceeds a time-varying tolerance,

$$\bar{\varepsilon}_q(t) = \frac{1}{n_q} \sum_{i=1}^{n_q} \|q_{t,i} - q_{t,i}^{\text{ref}}\| > \varepsilon_q(t),$$

where  $\varepsilon_q(t)$  is adaptively tightened according to the moving average of episode length (same scheme as [5]), yielding stricter thresholds as learning progresses. (ii) Base attitude deviation: let  $\omega_t = [\text{pitch}_t, \text{roll}_t]^\top$  and  $\omega_t^{\text{ref}} = [\text{pitch}_t^{\text{ref}}, \text{roll}_t^{\text{ref}}]^\top$  be the current and targeted robot root pitch/roll in the base frame; we terminate when

$$\|\omega_t\|_2 > 1.25 \|\omega_t^{\text{ref}}\|_2,$$

i.e., the current pitch/roll norm exceeds 1.25 $\times$  the reference. (iii) Self-collision: any detected self-contact (beyond a small tolerance) triggers termination.

*Reset.* At each reset we sample a start index from the entire reference trajectory (Sec. III-C), initialize the robot to the corresponding reference configuration and velocities, and add small random perturbations  $\varepsilon$  for robustness. Domain randomization is applied at episode start.

**Metrics.** Following [4], we report task/joint space errors averaged over time: global mean per-body position error  $E_{g\text{-}mpbpe}(\text{mm})$ , mean per-body position error  $E_{mpbpe}(\text{mm})$ , mean per-joint position error  $E_{mpjpe}(10^{-3}\text{rad})$ , and velocity variants  $E_{mpbve}(\text{mm/frame})$ ,  $E_{mpjve}(10^{-3}\text{rad/frame})$ .

## B. Ablations

We evaluate our method on long-horizon, high-dynamic motion (i.e., dance) tracking tasks. Two targeted ablations

are (i) the effectiveness of residual actions and (ii) the effectiveness of our sampling strategy.

**Ablations on Residual Actions.** We compare three variants: NONE (no residual; absolute commands; the Deep-Mimic recipe [1], [5], [4], [24], baseline), ALL (residual on all DOFs, I-CTRL fasion [12]), and SELECTIVE (residual on hip/knee pitch only; others pass through references; ours).

*Learning dynamics.* Fig. 5 shows the training returns. SELECTIVE exhibits the fastest improvement and the highest asymptote, while ALL learns faster than NONE but plateaus lower than SELECTIVE. NONE shows a pronounced early overshoot and subsequently stagnates at a substantially lower return, indicating poorer long-horizon credit assignment. These curves suggest that concentrating residual capacity on informative lower-body DoFs reduces action variance and prevents over-correction on already stable joints.

*Final accuracy.* Table I reports task- and joint-space errors (mean $\pm$ std). Relative to NONE, SELECTIVE reduces  $E_{g\text{-}mpbpe}$  by 15.7%,  $E_{mpbpe}$  by 18.2%,  $E_{mpjpe}$  by 20.5%, and  $E_{mpbve}$  by 4.3%;  $E_{mpjve}$  also decreases slightly ( $\sim$ 1.8%). Compared with ALL, SELECTIVE further improves  $E_{g\text{-}mpbpe}$  (11.7%),  $E_{mpbpe}$  (11.6%),  $E_{mpjpe}$  (9.6%), and  $E_{mpbve}$  (1.0%). The only exception is  $E_{mpjve}$ , where ALL is slightly lower, consistent with its more aggressive per-DoF corrections. Overall, SELECTIVE achieves the best or tied-best performance across metrics, indicating superior kinematic fidelity with comparable dynamical smoothness. These results support the hypothesis that selective residualization focuses learning on dynamics-sensitive joints, yielding better sample efficiency and long-horizon stability than applying residuals indiscriminately.

## Ablations on Sampling Strategy.

Difficulty based sampling strategies are usually employed for completing long-horizon motion tracking tasks [24], therefore we compare two convergent variants: *Failure* (Failure-Aware Priority Adaptation only; baseline) and *Failure+Balanced* (ours), which blends the online failure prior with offline distribution-aware balancing in the hip/knee pitch subspace (Sec. III-C).

*Results.* The learning curves in Fig. 6 show that *Failure+Balanced* achieves both faster improvement and higher asymptotic reward than *Failure*. In particular, the slope in the early regime is steeper and the plateau level is consistently higher, indicating better sample efficiency and reduced gradient noise. Qualitatively, the offline balancing equalizes coverage of rare pitch configurations, while the online failure prior focuses rollouts on persistently unstable windows; their combination avoids bias early and sustains progress later.

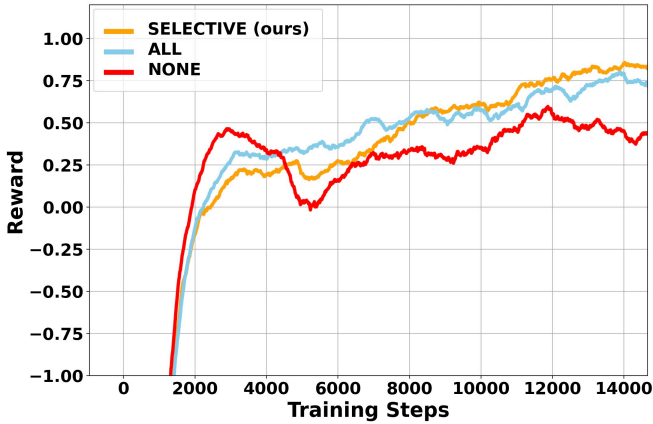


Fig. 5. Learning Curves under Residualization Strategies. Reward versus training steps for NONE, ALL, and SELECTIVE.

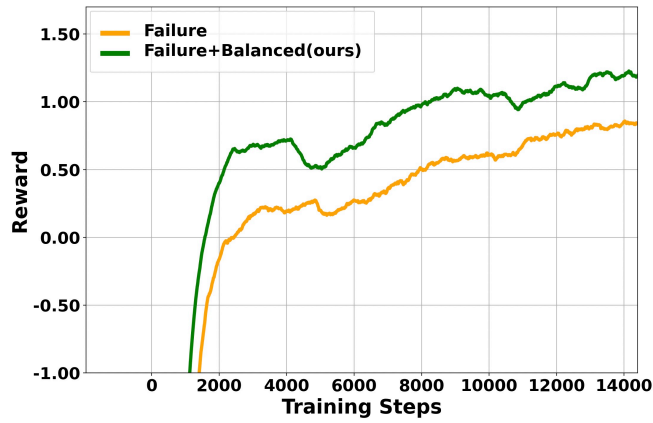


Fig. 6. Learning Curves for Sampling Ablations. Failure+Balanced converges faster and to a higher reward than Failure.

### C. Performance

We evaluated all dance sequences in total eight from [32]. The evaluation results are listed in Table II. These sequences are long-horizon ( $\approx 3$  min each) and highly dynamic, containing jumps, spins (up to  $360^\circ$ ), sprints, abrupt stops, and rapid transitions—challenging even for human performers. All policies are trained entirely in simulation with a single, unified configuration (observations, rewards, and hyperparameters) and without external perception or teacher models. After training, policies undergo sim-to-sim validation in MuJoCo; successful policies are then directly deployed to the real robot. Deployment framework follows an LCM-based pipeline [34] based on Walk-These-Ways [35], where the learned policy is exported to TorchScript and executed on the onboard Orin NX at 50 Hz. No test-time modifications are introduced (e.g., Kalman filtering of observations, PD gain retuning, and action rescaling); robustness is attained by the training procedure itself.

Across the dance sequences, the learned controller can track the long-horizon references (15K iterations training for every sequence is deployable). Qualitative rollouts (e.g., Fig. 2 (b) and (c)) illustrate high-dynamic behaviors such

TABLE II  
DANCE SEQUENCES EVALUATION.

Name (LAFANI)	Sim (MuJoCo)	Real (G1)
dance1_1	success <sup>1</sup>	success
dance1_2	success	success
dance1_3	success	success
dance2_1	success	untested <sup>2</sup>
dance2_2	success	untested
dance2_3	success	success
dance2_4	success	success
dance2_5	success	untested
walk1_1 <sup>3</sup>	[0, 50]s	—

1 “success” indicates full-sequence execution.

2 “untested” because of robot maintenance.

3 cross-motion: using the policy trained from dance1\_1.

as cartwheels, leaps, and fast heading changes. Sim-to-sim validation mirrors the real-robot behavior, indicating that dynamics compensation learned via residual actions transfers without per-sequence tuning.

### D. Cross-Platform Validation

For cross-platform validation, the same training recipe is applied to H1 and H1-2; both platforms reproduce high-dynamic behaviors qualitatively (see Fig. 2 (a) and (c)), confirming that the training pipeline and recipe using residual actions and our sampling scheme transfer across morphologies. To our knowledge, this is among early demonstrations of residual-action RL for tracking on long-horizon, highly dynamic motions across multiple humanoid platforms using a unified training paradigm.

## V. CONCLUSIONS

We presented a simple and scalable residual-action RL framework for humanoid motion tracking that achieves long-horizon, high-dynamic behaviors with a single-stage training recipe. By outputting residual actions on top of reference motions and coupling them with a distribution-/failure-aware sampling scheme, the controller reduces error accumulation, improves sample efficiency, and transfers zero-shot from simulation to real robots. We validated the approach primarily on Unitree G1 and further on H1/H1-2, demonstrating robust tracking of multi-minute dance sequences without task-specific retuning or test-time modifications.

**Key Observations.** (i) Cross-motion generalization. Policies trained with residual actions exhibit zero-shot transfer across motions: when applied to unseen but simpler references (e.g., walking, standing), the robot can track stably without additional tuning (Table II). Although the accuracy is lower than in-distribution dance sequences, this behavior indicates that the policy has internalized platform dynamics rather than memorizing motion-specific commands. (ii) Full-size hardware capability and limits. On full-size humanoids, the method enables high-dynamic tracking; however, torque-to-weight constraints remain a practical bottleneck (e.g., H1  $\sim 50$  kg with compute pack; H1-2  $\sim 80$  kg). Residualization reduces unnecessary actuation compared with absolute-

command baselines, yet peak torque margins still limit the amplitude and frequency of extreme maneuvers.

**Limitations and Future Work.** First, Our current selective residualization is hand-crafted. While effective, this heuristic may be suboptimal for other morphologies or motion families. We will replace manual selection with a model-based gating mechanism that lets the policy learn where residuals are needed. Second, we do not yet achieve general motion tracking across arbitrary references; our next goal is a unified humanoid behavior model that supports real-time tracking and genuinely whole-body teleoperation. Last, the current system is proprioception-only. Integrating visual perception will be essential for tasking the policy in unstructured environments and for environment-aware tracking (e.g., obstacle avoidance and terrain adaptation). Broader directions include energy-/safety-aware objectives, online system identification for rapid re-calibration, and richer motion libraries with automated retargeting. We believe these advances will further narrow the gap between reference motion and executable behavior on humanoids.

## REFERENCES

- [1] X. B. Peng, P. Abbeel, S. Levine, and M. Van de Panne, “Deepmimic: Example-guided deep reinforcement learning of physics-based character skills,” *ACM Transactions On Graphics (TOG)*, vol. 37, no. 4, pp. 1–14, 2018.
- [2] Z. Luo, J. Cao, J. Merel, A. Winkler, J. Huang, K. Kitani, and W. Xu, “Universal humanoid motion representations for physics-based control,” *arXiv preprint arXiv:2310.04582*, 2023.
- [3] C. Tessler, Y. Guo, O. Nabati, G. Chechik, and X. B. Peng, “Masked-mimic: Unified physics-based character control through masked motion inpainting,” *ACM Transactions on Graphics (TOG)*, vol. 43, no. 6, pp. 1–21, 2024.
- [4] W. Xie, J. Han, J. Zheng, H. Li, X. Liu, J. Shi, W. Zhang, C. Bai, and X. Li, “Kungfubot: Physics-based humanoid whole-body control for learning highly-dynamic skills,” *arXiv preprint arXiv:2506.12851*, 2025.
- [5] T. He, J. Gao, W. Xiao, Y. Zhang, Z. Wang, J. Wang, Z. Luo, G. He, N. Sobanbab, C. Pan *et al.*, “Asap: Aligning simulation and real-world physics for learning agile humanoid whole-body skills,” *arXiv preprint arXiv:2502.01143*, 2025.
- [6] M. Ji, X. Peng, F. Liu, J. Li, G. Yang, X. Cheng, and X. Wang, “Exbody2: Advanced expressive humanoid whole-body control,” *arXiv preprint arXiv:2412.13196*, 2024.
- [7] T. He, Z. Luo, X. He, W. Xiao, C. Zhang, W. Zhang, K. Kitani, C. Liu, and G. Shi, “Omnih2o: Universal and dexterous human-to-humanoid whole-body teleoperation and learning,” *arXiv preprint arXiv:2406.08858*, 2024.
- [8] Z. Fu, Q. Zhao, Q. Wu, G. Wetzstein, and C. Finn, “Humanplus: Humanoid shadowing and imitation from humans,” *arXiv preprint arXiv:2406.10454*, 2024.
- [9] Z. Chen, M. Ji, X. Cheng, X. Peng, X. B. Peng, and X. Wang, “Gmt: General motion tracking for humanoid whole-body control,” *arXiv preprint arXiv:2506.14770*, 2025.
- [10] K. Yin, W. Zeng, K. Fan, Z. Wang, Q. Zhang, Z. Tian, J. Wang, J. Pang, and W. Zhang, “Unitracker: Learning universal whole-body motion tracker for humanoid robots,” *arXiv preprint arXiv:2507.07356*, 2025.
- [11] Y. Wang, M. Yang, W. Zeng, Y. Zhang, X. Xu, H. Jiang, Z. Ding, and Z. Lu, “From experts to a generalist: Toward general whole-body control for humanoid robots,” *arXiv preprint arXiv:2506.12779*, 2025.
- [12] Y. Yan, E. V. Mascaro, T. Egle, and D. Lee, “I-ctrl: Imitation to control humanoid robots through constrained reinforcement learning,” *arXiv preprint arXiv:2405.08726*, 2024.
- [13] J. Y. Luo, Y. Song, V. Klemm, F. Shi, D. Scaramuzza, and M. Hutter, “Residual policy learning for perceptive quadruped control using differentiable simulation,” *arXiv preprint arXiv:2410.03076*, 2024.
- [14] S. Ross, G. Gordon, and D. Bagnell, “A reduction of imitation learning and structured prediction to no-regret online learning,” in *Proceedings of the fourteenth international conference on artificial intelligence and statistics*. JMLR Workshop and Conference Proceedings, 2011, pp. 627–635.
- [15] J. He, C. Zhang, F. Jenelten, R. Grandia, M. Bächer, and M. Hutter, “Attention-based map encoding for learning generalized legged locomotion,” *Science Robotics*, vol. 10, no. 105, p. eadv3604, 2025.
- [16] T. Zhang, B. Zheng, R. Nai, Y. Hu, Y.-J. Wang, G. Chen, F. Lin, J. Li, C. Hong, K. Sreenath *et al.*, “Hub: Learning extreme humanoid balance,” *arXiv preprint arXiv:2505.07294*, 2025.
- [17] T. Huang, J. Ren, H. Wang, Z. Wang, Q. Ben, M. Wen, X. Chen, J. Li, and J. Pang, “Learning humanoid standing-up control across diverse postures,” *arXiv preprint arXiv:2502.08378*, 2025.
- [18] I. Radosavovic, T. Xiao, B. Zhang, T. Darrell, J. Malik, and K. Sreenath, “Real-world humanoid locomotion with reinforcement learning,” *Science Robotics*, vol. 9, no. 89, p. eadi9579, 2024.
- [19] Z. Luo, J. Cao, K. Kitani, W. Xu *et al.*, “Perpetual humanoid control for real-time simulated avatars,” in *Proceedings of the IEEE/CVF International Conference on Computer Vision*, 2023, pp. 10895–10904.
- [20] Y. Ze, Z. Chen, J. P. AraÅšjo, Z.-a. Cao, X. B. Peng, J. Wu, and C. K. Liu, “Twist: Teleoperated whole-body imitation system,” *arXiv preprint arXiv:2505.02833*, 2025.
- [21] Y. Li, Y. Lin, J. Cui, T. Liu, W. Liang, Y. Zhu, and S. Huang, “Clone: Closed-loop whole-body humanoid teleoperation for long-horizon tasks,” *arXiv preprint arXiv:2506.08931*, 2025.
- [22] Q. Ben, F. Jia, J. Zeng, J. Dong, D. Lin, and J. Pang, “Homie: Humanoid loco-manipulation with isomorphic exoskeleton cockpit,” *arXiv preprint arXiv:2502.13013*, 2025.
- [23] J. Li, X. Cheng, T. Huang, S. Yang, R.-Z. Qiu, and X. Wang, “Amo: Adaptive motion optimization for hyper-dexterous humanoid whole-body control,” *arXiv preprint arXiv:2505.03738*, 2025.
- [24] T. E. Truong, Q. Liao, X. Huang, G. Tevet, C. K. Liu, and K. Sreenath, “Beyondmimic: From motion tracking to versatile humanoid control via guided diffusion,” *arXiv preprint arXiv:2508.08241*, 2025.
- [25] T. Johannink, S. Bahl, A. Nair, J. Luo, A. Kumar, M. Loskyll, J. A. Ojea, E. Solowjow, and S. Levine, “Residual reinforcement learning for robot control,” in *2019 international conference on robotics and automation (ICRA)*. IEEE, 2019, pp. 6023–6029.
- [26] Z. Xie, G. Berseth, P. Clary, J. Hurst, and M. Van de Panne, “Feedback control for cassie with deep reinforcement learning,” in *2018 IEEE/RSJ International Conference on Intelligent Robots and Systems (IROS)*. IEEE, 2018, pp. 1241–1246.
- [27] W. Sun, L. Feng, B. Cao, Y. Liu, Y. Jin, and Z. Xie, “Ulc: A unified and fine-grained controller for humanoid loco-manipulation,” *arXiv preprint arXiv:2507.06905*, 2025.
- [28] J. Schulman, F. Wolski, P. Dhariwal, A. Radford, and O. Klimov, “Proximal policy optimization algorithms,” *arXiv preprint arXiv:1707.06347*, 2017.
- [29] W. Xie, C. Bai, J. Shi, J. Yang, Y. Ge, W. Zhang, and X. Li, “Humanoid whole-body locomotion on narrow terrain via dynamic balance and reinforcement learning,” *arXiv preprint arXiv:2502.17219*, 2025.
- [30] J. Siekmann, Y. Godse, A. Fern, and J. Hurst, “Sim-to-real learning of all common bipedal gaits via periodic reward composition,” in *2021 IEEE International Conference on Robotics and Automation (ICRA)*. IEEE, 2021, pp. 7309–7315.
- [31] F. G. Harvey, M. Yurick, D. Nowrouzezahrai, and C. Pal, “Robust motion in-betweening,” *ACM Transactions on Graphics (TOG)*, vol. 39, no. 4, pp. 60–1, 2020.
- [32] H. Lv, “Lafan1 retargeting dataset (unitree g1/h1/h1-2),” Hugging Face, 2025. [Online]. Available: [https://huggingface.co/datasets/lvhaihang/LAFAN1\\_Retargeting\\_Dataset](https://huggingface.co/datasets/lvhaihang/LAFAN1_Retargeting_Dataset)
- [33] V. Nair and G. E. Hinton, “Rectified linear units improve restricted boltzmann machines,” in *Proceedings of the 27th International Conference on Machine Learning (ICML)*, 2010.
- [34] A. S. Huang, E. Olson, and D. C. Moore, “Lcm: Lightweight communications and marshalling,” in *Proceedings of the IEEE/RSJ International Conference on Intelligent Robots and Systems (IROS)*, 2010, pp. 4057–4062.
- [35] G. B. Margolis and P. Agrawal, “Walk these ways: Tuning robot control for generalization with multiplicity of behavior,” in *Conference on Robot Learning*. PMLR, 2023, pp. 22–31.